AMERICAN METEOROLOGICAL SOCIETY
AMS Journals Online

Full Text View

The Effects of Subgrid-Scale Parameterizations in a Zonally Averaged Ocean Model

Reto Knutti and Thomas F. Stocker

Climate and Environmental Physics, Physics Institute, University of Bern, Bern, Switzerland

Daniel G. Wright

Ocean Science Division, Bedford Institute of Oceanography, Dartmouth, Nova Scotia, Canada

ABSTRACT

Isopycnal diffusion and an additional transport velocity parameterizing the effect of mesoscale eddies are implemented in the ocean component of a 2.5-dimensional zonally averaged coupled ocean–atmosphere model. The equilibrium states of the coupled ocean–atmosphere model, resulting from the different mixing parameterizations, are compared, and extensive parameter sensitivity studies are presented. For the equilibrium base states, the new mixing schemes result in changes in the distributions of temperature and salinity that are significant in the Southern Ocean, where the isopycnal surfaces are steep and the eddy-induced transport velocity approximately cancels the Deacon cell. The temperature and salinity changes are relatively small in the rest of the ocean. Furthermore, the implementation of the new mixing schemes results in significant changes in the strength and the pattern of the thermohaline circulation. Transient responses of the coupled ocean–atmosphere system in global warming scenarios are compared for the different mixing parameterizations. It is demonstrated that large changes in the stability of the thermohaline circulation occur and that the observed changes in stability are highly parameter dependent.

1. Introduction

There is general agreement among physical oceanographers that the mixing processes in the ocean occur predominantly along neutral surfaces (i.e., surfaces of constant potential density with a local reference point; e.g., Iselin 1939;

Montgomery 1940; Redi 1982; McDougall 1987; Gent and McWilliams 1990).
These neutral surfaces are not horizontal in large parts of the ocean. The rapid mixing along neutral surfaces is generally referred to as isopycnal mixing, while the slower mixing across these surfaces is called diapycnal mixing (e.g., McDougall and Church 1986). For simplicity, ocean mixing has traditionally been parameterized as horizontal and vertical Fickian diffusion, with the vertical diffusivity taken to be smaller than the horizontal by several orders of magnitude. This approach has provided useful insights, but results in unrealistically large diapycnal diffusive fluxes in regions of steeply sloping neutral surfaces. To overcome this deficiency and improve the representation of mixing by unresolved eddies, new mixing parameterizations have been proposed in recent years (Redi 1982; Gent and McWilliams 1990).

To eliminate the unrealistically large diapycnal diffusive fluxes resulting from the horizontal/vertical diffusion parameterization, Redi (1982) presented a conceptual framework with the basic idea of aligning the diffusion tensor with the neutral surface by a coordinate rotation. Several implementations of this surrogate isopycnal diffusion have been published in recent years (e.g., Cox 1987; Hirst and Cai 1994), but for a long time attention has been detracted from these approaches because of computational inefficiency and the necessity of an additional horizontal background diffusivity to maintain numerical stability. A different idea is to formulate an ocean model in isopycnal coordinates instead of the traditional horizontal/vertical grid, but this does not completely solve the problem since neutral surfaces and surfaces of constant potential density may differ significantly, depending on the choice of the reference point (McDougall 1987).

Another major problem in most numerical ocean circulation models is their inability to adequately simulate the mixing effect of unresolved mesoscale eddies (i.e., typically, eddies with horizontal scales of tens of kilometers). Simple downgradient Fickian diffusion has been shown to be an inadequate representation of these effects (Gent et al. 1995). Since long integrations of eddy-resolving ocean models for the large-scale circulation are computationally unfeasible, the parameterization of eddy effects clearly needs to be improved. Unfortunately, it has proven difficult to accomplish this satisfactorily. Gent and McWilliams (1990, GM hereafter) proposed the introduction of an effective transport velocity for temperature, salinity, and tracers, consisting of the usual large-scale advection velocity plus a so-called eddy-induced transport velocity. This eddy-induced velocity represents the effect of a quasi-adiabatic stirring mechanism that conserves all tracer moments between isoneutral layers, yet systematically reduces the isoneutral slopes and therefore acts as a sink for available potential energy. This GM parameterization has been used in different ocean-only models (e.g., Danabasoglu et al. 1994; Gent et al. 1995; Robitaille and Weaver 1995; Danabasoglu and McWilliams 1995; Hirst and McDougall 1996; Duffy et al. 1997; Power and Hirst 1997; Hirst and McDougall 1998), as well as in coupled ocean–atmosphere models (e.g., Harvey 1995;Hirst et al. 1996; Gent et al. 1998; Wiebe and Weaver 1999; Hirst 1999; Gordon et al. 2000) with most of them reporting improvements in the spatial distribution of temperature salinity, and tracers compared to data, a decrease in the convection activity, more realistic circulation patterns in the Southern Ocean, and smaller model drift.

Recent theoretical work goes one step further and suggests the rotation of the diffusivity tensor for momentum as well as for scalars (McDougall and Church 1986; Greatbatch 1998) and improvements for the GM parameterization mentioned above (Griffies 1998).

The main purpose of this paper is to present new results on the impact of different mixing parameterizations on the ocean's thermohaline (i.e., temperature and salinity driven) circulation, the convection activity, and the distributions of temperature and salinity. Furthermore, extensive parameter studies and investigations on dynamical aspects and the stability of the thermohaline circulation for the different mixing parameterizations are presented. The main goal is not to identify absolute threshold values for the stability of the real ocean–atmosphere system, but to indicate how choices of mixing schemes and parameter values may affect the stability of the thermohaline circulation in three-dimensional models when global warming experiments are performed. We use the 2.5-dimensional zonally averaged coupled ocean–atmosphere model of Stocker et al. (1992b). This model captures the main features of the thermohaline circulation and has proven to be a useful simplification of more complex three-dimensional models, which are much more computationally expensive so that the number and duration of model integrations are limited.

This paper is organized as follows. In section 2 we briefly describe the model and the implementation of the new mixing parameterizations. The equilibrium states of the coupled ocean–atmosphere system are compared in section 3, and sensitivity studies are presented in section 4. In section 5 we focus on the stability of the thermohaline circulation in global warming experiments for the different mixing parameterizations. Finally, the results are discussed and summarized in section 6.

2. Model description

We use the 2.5-dimensional, zonally averaged 3-basin ocean model of Wright and Stocker (1991), with the closure scheme described by Wright et al. (1995, 1998). The ocean model is coupled to a one-dimensional, zonally and vertically averaged energy-balance model of the atmosphere (Stocker et al. 1992b) including an active hydrological cycle (Schmittner and Stocker 1999). The ocean model consists of three rectangular basins representing the Atlantic, Pacific, and Indian oceans, connected by an Antarctic circumpolar basin, the Southern Ocean. The model closure requires only the zonally averaged water mass properties across an ocean basin. Within the Southern Ocean, only one barrier to zonal flow is

included, so the zonal average is taken around the full longitudinal extent of the basin. The geometry is identical to that used by Stocker and Wright (1996). The model includes a simple thermodynamic sea ice component (Wright and Stocker 1993), but the seasonal cycle is neglected.

Three different parameterizations of mixing in the ocean are investigated: (i) the traditional horizontal/vertical diffusion scheme [see Wright and Stocker (1991) for details], referred to as HOR, which has been used in all previous experiments with this model; (ii) the isopycnal mixing scheme (ISO), where we use the straightforward approach of Redi (1982) and replace the horizontal and vertical diffusion terms in the equations for temperature, salinity, and biogeochemical tracers by isopycnal and diapycnal diffusion terms; and (iii) the Gent–McWilliams parameterization (GM), which is identical to ISO but with the large-scale advection velocity $\mathbf{u}$ replaced by the effective transport velocity $\mathbf{u}_{\mathrm{eff}}$, defined as the sum of the large-scale advection velocity and the eddy-induced transport velocity $\mathbf{u}^*$:

$$\mathbf{u}_{\mathrm{eff}} = \mathbf{u} + \mathbf{u}^*. \tag{1}$$

The eddy-induced transport velocity $\mathbf{u}^* = (\mathbf{v}^*, \ w^*)$ for the 2D model is given by

$$v^* = -\kappa s_z, \qquad w^* = \kappa s_y, \tag{2}$$

where $s = -\rho_y/\rho_z$ is the local isopycnal slope, ρ is the potential density and subscripts denote partial derivatives [y and z are the meridional and vertical coordinate, respectively (Gent et al. 1995)]; v^* and w^* are the meridional and vertical velocity components and κ is the Gent–McWilliams parameter (GM parameter: sometimes called isopycnal thickness diffusivity). Heat, salt, and biogeochemical tracers are advected by the effective transport velocity. A maximum value s_{max} is chosen for the slope s. If the slope exceeds the specified maximum value, it is simply set to the maximum value. This restriction has been commonly used to avoid very large vertical diffusive fluxes. For the model versions, ISO and GM, the changes due to vertical diffusion are calculated implicitly; no additional horizontal background diffusivity for numerical stability is necessary. Parameter settings are discussed in section 4; the parameter values for all experiments are listed in Table 1 .

The ocean model is spun up from rest for 5000 years by relaxing the surface values of temperature and salinity to the zonal and annual mean climatological data of Levitus et al. (1994) and Levitus and Boyer (1994) with a restoring timescale of 50 days. Wind stress based on observations (Han and Lee 1983) is applied at the ocean surface. After reaching a quasi-steady state under these restoring boundary conditions, the model is coupled to the atmosphere and integrated for a further 5000 years. The determination of the various atmospheric model parameters is discussed in detail in Stocker et al. (1992b).

3. Equilibrium states for the different mixing parameterizations

The equilibrium states of the coupled ocean–atmosphere system are now compared for the different mixing parameterizations. Parameter settings are listed in Table 1 . A constant value of 500 $\mathrm{m^2\ s^{-1}}$ for the GM parameter κ is assumed, but our main results do not depend on this choice. The important characteristics of the large-scale global circulation are reproduced with all three model versions. In Fig. 1 , the total Atlantic streamfunction (including the eddy-induced streamfunction) is shown. The Atlantic deep overturning (maximum Atlantic streamfunction below 1000 m) is about 24 Sv (Sv $\equiv 10^6\ \mathrm{m^3\ s^{-1}}$) for the model version HOR (Fig. 1a). For the ISO parameterization, the Atlantic cell is significantly stronger (28 Sv) and reaches deeper (Fig. 1b), whereas the GM parameterization leads to a weakening of the circulation cell (22 Sv) as well as a slight shoaling of the lower extremity of the North Atlantic Deep Water (NADW) flow (Fig. 1c). Previous results also indicated a decrease of the Atlantic overturning when introducing the GM parameterization (Danabasoglu and McWilliams 1995; Duffy et al. 1997). Duffy et al. (1997) conclude that the reduced diapycnal mixing in regions of steeply sloping isopycnal surfaces leads to the reduction of the Atlantic overturning. However, our results for the ISO mixing case indicate that the reduction of diapycnal mixing in regions of steeply sloping isopycnals actually strengthens the circulation. The reason for this is that density gradients in the region of deep-water formation are stronger due to reduced diapycnal mixing. The reduction of the Atlantic deep overturning evident in Fig. 1c is caused by the additional eddy-induced velocity in GM, which tends to flatten the isopycnals and hence to reduce meridional density gradients.

In the North Atlantic (see Fig. 1d) and North Pacific, the direct eddy-induced streamfunction shows small clockwise overturning cells in the uppermost 500 m, reaching maxima of 4 Sv and 2 Sv, respectively. These direct effects reinforce the basic overturning circulation in the North Atlantic. However, by design, the eddy-induced transport tends to flatten isopycnal surfaces and hence reduce horizontal density gradients. Thus, the eddy-induced transports always have a tendency to reduce the strength of the overturning circulation through their influence on the density field. The consequences of this overturning reduction are discussed below.

Major changes in the circulation pattern are observed in the Southern Ocean. The GM parameterization leads to the eddy-

induced contribution to the streamfunction shown in Fig. 1d ⊙. Note that the streamfunction in the Southern Ocean shows the sum over all grid boxes in the zonal direction. The anticlockwise overturning cell with a strength of about 20 Sv, located between 50° and 65°S and reaching from the ocean surface to a depth of about 3000 m, approximately cancels the so-called Deacon cell (Döös and Webb 1994) in the Southern Ocean, consistent with previous model experiments (e.g., Danabasoglu et al. 1994; Danabasoglu and McWilliams 1995; Hirst and McDougall 1998; Duffy et al. 1997). The Deacon cell is a model artefact that does not appear in eddy-resolving 3D models when the integration is performed along surfaces of constant density (Döös and Webb 1994). The elimination of this cell has a significant impact on biogeochemical tracer distributions in the Southern Ocean (e.g., Robitaille and Weaver 1995;Duffy et al. 1997; England and Holloway 1998).

The temperature distributions in the Atlantic and Southern Ocean obtained with the different mixing parameterizations are compared with the zonally averaged data of Levitus and Boyer (1994) (Fig. 2 ⊙). The agreement with the data is similar for all model versions. Again, the main difference is observed in the Southern Ocean, where the parameterizations ISO and GM show strong horizontal, but very weak vertical temperature gradients. The latter characteristic can be explained by the strength of the vertical component of the isopycnal diffusive flux, which exceeds the explicit vertical diffusive flux in the HOR version by several orders of magnitude. All Geophysical Fluid Dynamics Laboratory-based results obtained under restoring boundary conditions indicate cooling in the range of 0.3° to 3°C in the Southern and deep ocean (Danabasoglu et al. 1994; Hirst and Cai 1994; Robitaille and Weaver 1995;Hirst and McDougall 1996; Duffy et al. 1997) when the new mixing scheme is introduced. Duffy et al. (1997) attributed this cooling to changes in advection and convection as well as to changes in diffusive fluxes. They find that increased vertical diffusive mixing in the regions of steeply sloping isopycnal surfaces in the Southern Ocean increases the heat loss of the Southern Ocean to the cold high-latitude atmosphere. In contrast to this, Danabasoglu and McWilliams (1995) observed a sharp decrease in the heat loss of the Southern Ocean for the improved mixing, and they attribute the cooling of the Southern and deep ocean to a reduction in poleward oceanic heat transport and a reduction in deep convection. While Duffy et al. (1997) concluded that the cooling of the Southern and deep oceans may be generic to isopycnal mixing parameterizations, we do not observe such a cooling in the results of our 2.5D model. In our experiments the heat loss to the atmosphere in the region of the Southern Ocean is higher for ISO and GM by a factor of 2, but we observe only a slight cooling of the Southern Ocean. The deep ocean remains essentially unchanged, except for the ISO version where a slight warming due to stronger North Atlantic Deep Water formation occurs (Fig. 2b ⊙). In agreement with our results, Harvey (1995) finds only minor differences in the temperature and salinity distributions with a simplified coupled ocean–atmosphere model. The increased heat loss from the Southern Ocean affects the local temperature distribution, but the temperature of the deep ocean in the rest of the basin is essentially controlled by the ratio of colder Antarctic Bottom Water (AABW) formation to warmer NADW formation.

Figure 3 ⊙ shows the salinity distribution in the Atlantic and Southern Oceans for the different model versions and the zonally averaged data of Levitus et al. (1994). The increased high-latitude downward diffusion in ISO and GM obviously leads to significant changes in the salinity distribution in the Southern Ocean as well as changes in the deep Pacific and Indian Oceans. A general freshening tendency is observed in these basins, consistent with previous model results (Hirst and Cai 1994). The isopycnal surfaces act as pathways along which the fresh surface water may mix into the ocean interior, and we therefore observe a stronger salinity minimum at 50°S reaching to a depth of about 1000 m for the ISO and GM versions (Figs. 3b and 3c ⊙). The results of the stronger isopycnal diffusion and reduced horizontal diffusion in the ISO version compared to HOR are also observed in the density distribution (Fig. 4 ⊙). Compared to the ISO version, the additional eddy mixing in the GM version slightly depletes the slope of the isopycnal surfaces (Fig. 4c ⊙).

The distributions of water masses formed at different locations reveal further characteristics of the mixing parameterizations. In the uppermost 1000 m at intermediate and low latitudes only small differences can be identified, but differences are larger in the deep ocean. In the ISO model version there is a very distinct separation of NADW and AABW. For example, in some locations where the Atlantic meets the Southern Ocean, the relative contribution of NADW to the total water mass decreases from 80% to 20% within 5° of latitude. Also, the outflow of NADW to the Pacific and Indian Ocean for ISO and GM is reduced by at least a factor of 2 compared to HOR. These changes in the water mass boundaries can be explained by the reduced diapycnal mixing in the region of steep isopycnal surfaces in the Southern Ocean. In this respect, the ISO version produces unrealistic results. The introduction of the eddy-induced velocity as an additional mixing mechanism in GM significantly improves the situation by reducing the horizontal gradients in water mass properties.

An even more important aspect of the GM parameterization is the reduction of the convection activity (see also section 4) in the North Atlantic and Southern Ocean compared to HOR and ISO. Similar results have been reported in detail by previous investigators (e.g., Danabasoglu et al. 1994; Danabasoglu and McWilliams 1995; Hirst and McDougall 1996; Duffy et al. 1997). The tendency of the GM parameterization to flatten isopycnals reduces the development of static instabilities in large parts of the ocean, while vertical heat and salt fluxes continue to be maintained by isopycnal mixing. Instantaneous convective mixing is therefore reduced and replaced by a physically more appropriate mechanism.

4. Parameter sensitivity studies

Extensive sensitivity tests were performed under restoring boundary conditions for the GM parameterization to determine the influence of the various parameters used in this mixing formulation. As a reference state, we take the solution under

restoring boundary conditions obtained with the parameters given in Table 1 ⊙. The differences of the reference state from the coupled GM equilibrium state, as described in detail in section 3, are small. Starting with the reference state, the values for the isopycnal diffusivity K_I, diapycnal diffusivity K_D, GM parameter κ, maximum isopycnal slope s_{max}, and several other parameters were systematically changed and a 5000-yr spinup from rest was performed for each parameter set. The qualitative dependencies discussed in this section are not affected by the choice of κ.

a. Isopycnal diffusivity

In large parts of the ocean, the isopycnal surfaces are approximately horizontal and the isopycnal/diapycnal diffusivities in ISO have essentially the same effect as the horizontal/vertical diffusivities in HOR. A value of 1000 m^2 s^{-1} for the horizontal diffusivity K_H is consistently used in almost all ocean models for depth-independent K_H, and the same value may therefore also be appropriate for the isopycnal diffusivity K_I (e.g., Lin 1988; Gerdes et al. 1991; Hirst and Cai 1994; Danabasoglu and McWilliams 1995; Hirst and McDougall 1996; Duffy et al. 1997; Weaver and Eby 1997). We varied K_I in the range of 100 to 5000 m^2 s^{-1} (13 values) and observed changes in the temperature and salinity distribution due to the changes in the diffusive fluxes. However, the overall solution of the model changes little, and no clear trends can be observed. For example, the maximum Atlantic deep overturning varies by less than 1 Sv for the different values of K_I. Values in the range of about 500 to 2000 m^2 s^{-1} seem to be suitable for model purposes.

b. Diapycnal diffusivity

Values in the range of 10^{-5} to 10^{-4} m^2 s^{-1} are generally used in ocean models for vertical and diapycnal diffusivities. Tracer experiments indicate the same range, but large spatial variations are known to occur (Ledwell et al. 1993; Toole et al. 1994). Some authors have tried to take spatial variations into account by choosing depth-dependent values (e.g., Hirst and Cai 1994; Hirst and McDougall 1996); others used a medium range constant value of 5×10^{-5} m^2 s^{-1} (e.g., Danabasoglu et al. 1994; Danabasoglu and McWilliams 1995; Duffy et al. 1997). Here we consider a spatially uniform diapycnal diffusivity K_D and examine the model sensitivity to variations in this parameter over the range 10^{-5} to 10^{-4} m^2 s^{-1} (10 values). The model results show a distinct and strong dependence on K_D, very similar to the dependence on the vertical diffusivity K_V found in previous studies with HOR (Wright and Stocker 1992). In low latitudes, enhanced diapycnal diffusion increases the vertical diffusive heat flux into the deep ocean, which results in a larger meridional density gradient. This strengthens the circulation and increases the large-scale meridional transports. In the range mentioned above, the Atlantic deep overturning increases from 8 to 23 Sv, the maximum Atlantic meridional heat flux increases from 0.8 to 1.3 PW, and the maximum Atlantic meridional freshwater flux increases from 0.15 to 0.23 Sv with increasing K_D. The Atlantic deep overturning, shown in Fig. 5 ⊙, is approximately proportional to $(K_D)^{0.5}$, consistent with scaling arguments and with the results of Wright and Stocker (1992) who found very similar dependencies for the Atlantic overturning on the vertical diffusivity K_V [Atlantic deep overturning proportional to $(K_V)^{0.46}$]. We therefore conclude that, at least in our model, the diapycnal diffusivity in the GM model version has essentially the same influence and importance as the vertical diffusivity in the HOR model version.

c. GM parameter

The Gent–McWilliams parameter κ is not a physically measurable quantity; its value must be determined by comparing model results with observations. A constant value of 1000 m^2 s^{-1} has been used in most previous experiments (Gent et al. 1995; Danabasoglu and McWilliams 1995; Danabasoglu et al. 1994; Hirst and McDougall 1996; Weaver and Eby 1997), but the uncertainty is large, and spatial variations are indicated when κ is estimated from numerical model results and theoretical ideas (Hirst and McDougall 1996; Visbeck et al. 1997). The choice of a basinwide constant value is assumed for simplicity; further knowledge and estimates from data and models are necessary to overcome this deficiency. We investigated the range of κ from 100 to 5000 m^2 s^{-1} (13 values). The results are plotted in Fig. 6 ⊙. The minimum Atlantic and Southern Ocean eddy-induced streamfunction, which indicates the strength of the counterclockwise eddy-driven circulation cell in the Southern Ocean (see Fig. 1d ⊙), decreases linearly from −4 to about −45 Sv when κ is increased from 100 to 1000 m^2 s^{-1}. The linear dependence is as expected from Eq. (2) if no feedback mechanisms are present. When κ is increased further, the minimum eddy-induced streamfunction continues to decrease, but more slowly than a linear extrapolation would suggest (Fig. 6a ⊙). This is due to the negative feedback of the eddy-induced transport reducing the isopycnal slopes, which acts to reduce the magnitude of the eddy-induced transport.

The eddy-induced streamfunction has a strong impact on the model's behavior. The maximum Atlantic overturning shows a strong dependence on κ and decreases from 26 to 8 Sv when κ is increased from 100 to 5000 m^2 s^{-1} (Fig. 6b ⊙). The reduction of the Atlantic overturning leads to a severe decrease of the maximum Atlantic meridional heat flux from about 1.4 PW to 0.9 PW. For the reference run ($\kappa = 1000$ m^2 s^{-1}), a value of about 1.1 PW is obtained, in good agreement with observations (Hall and Bryden 1982; Trenberth and Solomon 1994). The fraction of convecting cells is reduced by almost an order of magnitude (Fig. 6c ⊙), and the convection depth in the northernmost Atlantic cell (measured downward from the ocean surface) is reduced by about a factor of 3 (Fig. 6d ⊙). These results reflect the fact that the eddy-induced velocity represents a stirring mechanism that tends to flatten the isopycnals and reduce horizontal density gradients, hence reducing the overturning circulation. The tendency to flatten isopycnals also tends to prevent the development of static instabilities, especially in regions of deep-water formation. Consequently, convective mixing is drastically reduced. Further details will be discussed in section 5 where we will demonstrate that an increasing value of κ also reduces the stability of the thermohaline circulation.

d. Maximum isopycnal slope

The value used to limit the maximum isopycnal slope, s_{max}, has been chosen differently in different model studies, ranging between 10^{-3} (Gent et al. 1995) and 10^{-2} (Hirst and Cai 1994; Danabasoglu and McWilliams 1995). In our model, numerical behavior and computational efficiency are improved when s_{max} is reduced. However, it is important to choose s_{max} sufficiently large that its value does not strongly influence the model solution. We varied the value of s_{max} in the aforementioned range and found that a value of 2×10^{-3} is large enough not to restrict the model results. That is, choosing s_{max} any larger does not significantly change the model's steady state solution. As an example, Fig. 7 ⊙ shows that the maximum Atlantic deep overturning is only weakly influenced when the maximum isopycnal slope is increased beyond 2×10^{-3}. This result is consistent with the observation of Hirst and McDougall (1996) that their model solution showed only small changes when the maximum slope was limited to 2×10^{-3}.

5. Stability of the thermohaline circulation

The stability of the thermohaline circulation is a central problem in climate dynamics, but a systematic investigation of stability properties as a function of mixing parameters used in ocean models has not been done. As a step in this direction, we consider the stability of the modern steady-state circulation corresponding to the different model versions in response to projected global warming. The mechanisms and the general behavior of the different model versions have been confirmed by various freshwater experiments (Knutti 1999), which we do not reproduce here.

Stocker and Schmittner (1997) showed that the model exhibits threshold values in global warming scenarios, above which the NADW formation stops and never recovers, and that these threshold values depend on the rate of increase of the warming. Following Schmittner and Stocker (1999), such scenarios are simulated here by assuming an exponential increase of the atmospheric CO_2 concentration with time:
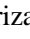
$$pCO_2(t) = (280 \text{ ppmv})e^{\gamma t}, \qquad (3)$$

where γ is the rate of CO_2 increase. Once a prescribed level is reached, the CO_2 concentration is held constant and the integration is continued. The relation between the CO_2 concentration and the additional radiative forcing ΔF at the top of the atmosphere is parameterized according to Shine et al. (1995):

$$\Delta F(t) = \Delta F_{2\times} \ln\left(\frac{pCO_2(t)}{280 \text{ ppmv}}\right) \Big/ \ln(2)$$

$$= \Delta F_{2\times} \frac{\gamma}{\ln(2)}t. \qquad (4)$$

The parameter $\Delta F_{2\times}$ denotes the additional radiative forcing for a doubling of CO_2, its value is fixed at 7.3 W m^{-2}, which corresponds to a global equilibrium temperature increase of about 3.7°C in our model. The albedo is kept constant, advection velocities in the atmosphere are diagnosed when negative diffusivities occur in the atmosphere, and the zonal distribution of precipitation is held constant in time [see Schmittner and Stocker (1999) and Schmittner et al. (2000b) for details]. For a

given end level of ΔF or pCO_2, a global warming scenario is integrated until a new equilibrium state is established (usually 1000 years). We then examine the change in NADW formation to determine the critical forcing or critical CO_2 value beyond which the NADW formation stops and does not recover. This value is determined over a broad range of γ, the rate of increase of radiative forcing.

It may be tempting to interpret the results in this section as absolute threshold values in terms of CO_2 concentrations applicable for climate predictions, but this would be inappropriate. The model used for this study is too simple to decide whether a threshold for a collapse of the Atlantic thermohaline circulation exists for the real ocean–atmosphere system or to determine the value of such a threshold. Most ocean–atmosphere models show a reduction of North Atlantic deep-water formation in global warming experiments, and there is evidence from models that there may be a threshold value for global warming beyond which the North Atlantic thermohaline circulation completely stops and does not recover (e.g., Manabe and Stouffer 1994). In contrast to this, Latif et al. (2000) recently found that global warming has almost no net influence on the Atlantic thermohaline circulation. This is due to compensating stabilizing effects caused by more frequent El Niño regimes, which influence the surface freshwater balance of the tropical Atlantic (Schmittner et al. 2000a). Improved models may answer this discrepancy in the future. Our intention here is to investigate mechanisms and dynamical aspects of abrupt reorganizations as well as to identify whether changes in parameter settings or the choice of a different mixing parameterization might stabilize or destabilize the thermohaline circulation. Climate predictions and absolute threshold values must, if they exist for the real climate system, be investigated with more comprehensive (and computationally more expensive) coupled 3D ocean–atmosphere models.

The critical forcing for an Atlantic circulation collapse was calculated for different rates of increase of the radiative forcing, starting from the coupled equilibrium states described in section 3. Figure 8 ◑ shows the results for HOR, ISO, GM, and the results of the corresponding model version published in Schmittner and Stocker (1999). The differences between the latter and HOR are due to slightly different parameter settings, updated surface restoring conditions, and an improved calculation for seawater density (Wright 1996). The critical forcing in the new model versions ISO and GM shows the same qualitative dependence on the forcing increase rate as found with the HOR mixing scheme. It is almost constant for higher increase rates (>0.1 W m^{-2} yr^{-1}) and becomes larger for smaller increase rates (<0.1 W m^{-2} yr^{-1}) because the ocean is given more time to absorb the additional heat and freshwater. For each version, a threshold for the increase rate exists below which the NADW formation always recovers (values for ΔF up to 50 W m^{-2} have been tested). Figure 8 ◑ shows that values of the critical forcing depend on the mixing parameterization. The ISO parameterization shows much higher critical forcing values than HOR and GM, indicating that the ISO version is less sensitive to perturbations in the heat budget. However, we will show later in this section that the absolute position of the GM curve is highly dependent on the GM parameter κ.

In section 4 we showed that the Atlantic overturning is stronger for higher values of the diapycnal diffusivity. This statement is true for all mixing parameterizations. A stronger overturning is usually less sensitive to perturbations, and one would therefore expect higher values for the critical forcing. To test this hypothesis, the critical forcing was calculated iteratively as described above for values of K_V and K_D in the range of 3×10^{-5} to 10^{-4} m^2 s^{-1}. For simplicity, the forcing increase rate was fixed at a value of 0.1 W m^{-2} yr^{-1}. The results are shown in Fig. 9 ◑. Note that the parameter q_{SO} controlling the Southern Ocean deep-water formation is 0.5 Sv instead of 0.3 Sv in the following experiments, but the qualitative results do not depend on this choice. Briefly, to account for the effect of brine rejection around Antarctica, a fraction of the salt ejected during sea ice formation is mixed with a specified volume of surface water and slotted into the water column at its stability level before applying the usual convection scheme based on instantaneous mixing. Here q_{SO} denotes the flux of water to go into plumes. A more detailed description can be found in Stocker and Wright (1996).

A strong dependence of the critical forcing on the diapycnal/vertical diffusivity is found for HOR and GM as expected. For these two parameterizations, the critical forcing increases by about an order of magnitude when the diapycnal/vertical diffusivity is increased from 3×10^{-5} to 10^{-4} m^2 s^{-1}. However, for ISO, no dependence is found in our model, even though the Atlantic overturning increases from 23 to 31 Sv when the diapycnal diffusivity K_D is increased in the above range. Mechanisms that could explain this observation are discussed below.

Overturning is essentially controlled by the vertical density structure in the North Atlantic. It reduces and eventually stops when a fresh and warm water pool establishes in the surface region of the North Atlantic as a result of increasing atmospheric temperatures and net precipitation. The isopycnal surfaces in the North Atlantic are steepest in the ISO version. This results in locally high vertical diffusivities that contribute strongly to the dilution of heat and salt anomalies and thus lead to a generally higher level of the critical forcing. The horizontal diffusivities in the uppermost 500 m of the North Atlantic, on the other hand, are small and compete with the strong horizontal advection. We suggest, therefore, that the horizontal mixing in the surface North Atlantic is largely controlled by advection and that changes in the diapycnal diffusion play a minor role (in our model).

Using the GM scheme, the isopycnal slopes are reduced by the eddy-induced advection, and the horizontal component of the isopycnal diffusivity therefore increases. Additionally, for the GM version, the horizontal advection in this region is smaller than in the ISO version (difference: 5 to 8 Sv, depending on K_D) decreasing further the relative importance of advection versus K_D. Because of the reduced isopycnal slope, primarily changes in K_D largely affect the vertical diffusive fluxes. The qualitative behavior of the GM version therefore resembles the behavior of the HOR version.

When focusing on the meridional overturning strength of all model runs in Fig. 9 ⊙, a second argument arises to explain the differences in the transient response of the different model versions. For small diapycnal/vertical diffusivities, the Atlantic overturning strength is generally small but varies for the different model versions (range: 14–23 Sv for $K_D = 3 \times 10^{-5}$ m^2 s^{-1}). Large differences in the stability of the thermohaline circulation are therefore not surprising. On the other hand, the relative variations in the overturning strength are much smaller for large diapycnal/vertical diffusivities (range: 27–31 Sv for $K_D = 10^{-4}$ m^2 s^{-1}). Consistent with this, the variations in the critical forcing are much smaller for large diapycnal/vertical diffusivities. Additional experiments with a higher maximum isopycnal slope $s_{max} = 0.01$ show an increase of the critical forcing in the ISO version by about 30%, but still no dependence on the diapycnal diffusivity is observed.

Note also that the interpretation of the stability as a function of mixing parameters (Fig. 9 ⊙) is generally more difficult than if the dependence on the forcing parameters is investigated (Fig. 8 ⊙). While for the latter all transient experiments start from an identical steady state of the coupled ocean–atmosphere system, experiments with varying diffusivities require their individual equilibrium state for each point plotted in Fig. 9 ⊙. Numerical aspects in the spinup phase or variations in atmospheric parameters (diagnosed at the time of coupling ocean and atmosphere) are therefore likely to affect the transient behavior in the global warming scenarios.

In a final set of experiments, the sensitivity of the critical forcing to changes in the GM parameter κ was investigated. In Fig. 10 ⊙, the critical forcing is plotted versus κ for the standard GM model version and a parameterization with reduced deep-water formation in the Southern Ocean (GM2; see Table 1 ⊙ for details). In either case, a strong decrease of the stability is observed for increasing values of κ. Indeed, for sufficiently large values of κ, the system is close to a bifurcation point where NADW formation tends to stop even without introducing any perturbation. This sensitivity is qualitatively consistent with the results of Stocker et al. (1992a) who demonstrate the sensitivity of the overturning circulation to the buoyancy contrast between the Southern Ocean and the North Atlantic. As κ is increased, there is increased tendency for AABW to penetrate into the Atlantic basin as a result of the "anticlockwise" overturning circulation in the Southern Ocean associated with the GM eddy-mixing scheme. It seems likely that this increased Antarctic influence is the primary reason for the reduced stability of the NA overturning circulation. To further investigate this possibility, additional experiments were done with the GM parameterization limited to the regions south or north of 40°S. Results with the GM scheme applied only in the Southern Ocean were similar to those before, while those with the GM scheme applied only outside of the Southern Ocean gave results more like those obtained with the ISO formulation. This emphasizes the importance of changes in circulation in the Southern Ocean.

Apparently, the increased AABW influence with increasing κ reduces the stability of the Atlantic overturning by shifting the system closer to a bifurcation point. We note that the results of Stocker et al. (1992a) illustrate that, even in the presence of multiple equilibria, it is possible for the ocean system to make a smooth transition between the modern state and a "glacial" state with increased AABW influence in the Atlantic basin. The results presented here indicate that, while such a smooth transition is possible, the glacial state is less stable to buoyancy perturbations, at least in the present model. Qualitatively similar behavior was found in a 3D ocean general circulation model (Tziperman 1997).

The above results and results such as those presented by Marotzke and Stone (1995) emphasize the importance of improving our knowledge regarding the parameter sensitivities in numerical models used to make climate change predictions. Although the use of flux corrections [e.g., Sausen et al. (1988)] may avoid unrealistic climate drift when oceanic and atmospheric models are coupled, such approaches do not address the underlying model inadequacies. Climate change predictions based on a climate model whose initial state appears realistic, but is positioned unrealistically close to a mode transition are clearly unreliable. Determination of model parameter sensitivities for complex 3D models is a daunting task, but it will be an important step towards insuring model sensitivities consistent with those of the real world.

6. Conclusions

We investigated the impact of isopycnal mixing and the GM parameterization in a 2.5D zonally averaged, coupled ocean–atmosphere model. It has been found that each of the mixing parameterizations is able to reproduce the large-scale modern circulation pattern as well as the spatial distribution of temperature, salinity, meridional fluxes, evaporation, and precipitation.

The reduced diapycnal mixing in the ISO version of the model leads to very abrupt transitions between water masses,

reflecting that the mixing mechanism that depletes density gradients has been reduced in strength, particularly in regions of strongly sloping isopycnals. The stability of the circulation for the ISO formulation is essentially independent of the diapycnal diffusivity and therefore also insensitive to the changes in overturning strength over this range of diffusivities in the ISO formulation. Changes in other parameters also hardly affect the stability of this model version. However, we note that the results obtained with the ISO version are significantly modified when the model is extended to the GM version, which includes a representation for the eddy-induced transport. This transport provides an additional mixing mechanism to limit isopycnal steepening. The consequences include a drastic decrease of the convective adjustment activity, a significant weakening of the large-scale circulation, and a much higher tendency for major changes or reorganizations of the circulation.

The GM version appears to give the most realistic results of the three formulations considered. In particular, a more realistic circulation in the Southern Ocean is achieved through the cancellation of the Deacon cell, which should improve the model's capability to correctly simulate distributions of biogeochemical tracers and the carbon cycle in that region. The use of the GM parameterization in future experiments is recommended, although in our case numerical handling, especially when coupling the ocean to the atmosphere, is not as easy as in the traditional HOR version, at least in our model.

Parameter dependencies of all three model versions were investigated and several important results regarding the stability of the modern circulation were obtained. First, the stability of the thermohaline circulation is highly dependent on parameter settings and on which mixing parameterization is used. Similar behavior is likely to occur in other more comprehensive ocean–atmosphere models, although the computational expense of these models will make it prohibitively expensive to determine detailed dependencies.

Second, the strength of the thermohaline circulation does not necessarily determine its stability in response to perturbations in the heat and freshwater budgets. This conclusion is supported by Fig. 10 ⊙, where (i) the critical forcing for the GM2 version lies below 2 W m^{-2} for high values of κ, although a strong Atlantic overturning of more than 20 Sv is detected, and (ii) for small κ the GM2 version is less stable than the standard GM version, even though the Atlantic overturning of GM2 is 5 Sv stronger. Figure 9 ⊙ also supports this conclusion as it shows that the critical forcing for the ISO version is approximately constant although the Atlantic overturning increases significantly when the diapycnal diffusivity is increased.

Third, the fact that the critical forcing is higher for smaller rates of CO_2 increase is a robust result that is not affected by any parameter setting or by the mixing parameterization. However, as illustrated by Fig. 8 ⊙, absolute threshold values for a circulation collapse in terms of CO_2 concentrations or radiative forcing values are very difficult to estimate. We emphasize that the purpose of the experiments presented here is not to give realistic absolute threshold values, but to investigate mechanisms and dependencies that contribute to a better understanding of the ocean–atmosphere system. Further experiments with more comprehensive models are required to better understand the relevance of our results for the real world.

REFERENCES

Cox, M. D., 1987: Isopycnal diffusion in a z-coordinate ocean model. *Ocean Modelling* (unpublished manuscripts), **74,** 1–5.

Danabasoglu, G., and J. C. McWilliams, 1995: Sensitivity of the global ocean circulation to parameterizations of mesoscale tracer transports. *J. Climate,* **8,** 2967–2987. Find this article online

——, ——, and P. R. Gent, 1994: The role of mesoscale tracer transports in the global ocean circulation. *Science,* **264,** 1123–1126.

Döös, K., and D. J. Webb, 1994: The Deacon cell and the other meridional cells of the Southern Ocean. *J. Phys. Oceanogr.,* **24,** 429–442. Find this article online

Duffy, P. B., K. Caldeira, J. Selvaggi, and M. I. Hoffert, 1997: Effects of subgrid-scale mixing parameterizations on simulated distributions of natural ^{14}C, temperature, and salinity in a three-dimensional ocean general circulation model. *J. Phys. Oceanogr.,* **27,** 498–523. Find this article online

England, M. H., and G. Holloway, 1998: Simulation of CFC content and water mass age in the deep North Atlantic. *J. Geophys. Res.,* **103,** 15 885–15 901.

Gent, P. R., and J. C. McWilliams, 1990: Isopycnal mixing in ocean circulation models. *J. Phys. Oceanogr.,* **20,** 150–155. Find this article online

—— , J. Willebrand, T. J. McDougall, and J. C. McWilliams, 1995: Parameterizing eddy-induced tracer transports in ocean circulation models. *J. Phys. Oceanogr.,* **25,** 463–474. Find this article online

—— , F. O. Bryan, G. Danabasoglu, S. C. Doney, W. R. Holland, W. G. Large, and J. C. McWilliams, 1998: The NCAR climate system model ocean component. *J. Climate,* **11,** 1278–1306. Find this article online

Gerdes, R., C. Köberle, and J. Willebrand, 1991: The influence of numerical advection schemes on the results of ocean general circulation models. *Climate Dyn.,* **5,** 211–226.

Gordon, C., C. Cooper, C. A. Senior, H. Banks, J. M. Gregory, T. C. Johns, J. F. B. Mitchell, and R. A. Wood, 2000: The simulation of SST, sea ice extents and ocean heat transports in a version of the Hadley Centre coupled model without flux adjustments. *Climate Dyn.,* **16,** 147–168.

Greatbatch, R. J., 1998: Exploring the relationship between eddy-induced transport velocity, vertical momentum transfer, and the isopycnal flux of potential vorticity. *J. Phys. Oceanogr.,* **28,** 422–432. Find this article online

Griffies, S. M., 1998: The Gent–McWilliams skew flux. *J. Phys. Oceanogr.,* **28,** 831–841. Find this article online

Hall, M. M., and H. L. Bryden, 1982: Direct estimates and mechanisms of ocean heat transport. *Deep-Sea Res.,* **29,** 339–359.

Han, Y. J., and S. W. Lee, 1983: An analysis of monthly mean windstress over the global ocean. *Mon. Wea. Rev.,* **111,** 1554–1566. Find this article online

Harvey, L. D. D., 1995: Impact of isopycnal diffusion on heat fluxes and the transient response of a two-dimensional ocean model. *J. Phys. Oceanogr.,* **25,** 2166–2176. Find this article online

Hirst, A. C., 1999: The Southern Ocean response to global warming in the CSIRO coupled ocean–atmosphere model. *Environ. Model. Software,* **14,** 227–241.

—— , and W. Cai, 1994: Sensitivity of a World Ocean GCM to changes in subsurface mixing parameterization. *J. Phys. Oceanogr.,* **24,** 1256–1279. Find this article online

—— , and T. J. McDougall, 1996: Deep-water properties and surface buoyancy flux as simulated by a *z*-coordinate model including eddy-induced advection. *J. Phys. Oceanogr.,* **26,** 1320–1343. Find this article online

—— , and —— , 1998: Meridional overturning and dianeutral transport in a *z*-coordinate ocean model including eddy-induced advection. *J. Phys. Oceanogr.,* **28,** 1205–1223. Find this article online

—— , H. B. Gordon, and S. P. O'Farell, 1996: Global warming in a coupled climate model including oceanic eddy-induced advection. *Geophys. Res. Lett.,* **23,** 3361–3364.

Iselin, C. O., 1939: The influence of vertical and lateral turbulence on the characteristics of the waters at mid-depths. *Trans. Amer. Geophys. Union,* **20,** 414–417.

Knutti, R., 1999: Parametrisierungen von sub-skaligen Mischungsprozessen in einem zonal gemittelten Ozean-Modell. M.S. thesis, Dept. of Climate and Environmental Physics, Physics Institute, University of Bern, Bern, Switzerland, 143 pp. [Available from Climate and Environmental Physics, Physics Institute, University of Bern, Sidlerstrasse 5, CH-3012 Bern, Switzerland.].

Latif, M., E. Roeckner, U. Mikolajewicz, and R. Voss, 2000: Tropical stabilization of the thermohaline circulation in a greenhouse warming simulation. *J. Climate,* **13,** 1809–1813. Find this article online

Ledwell, J. R., A. J. Watson, and C. S. Law, 1993: Evidence for slow mixing across the pycnocline from an open-ocean tracer-release experiment. *Nature,* **364,** 701–703.

Levitus, S., and T. P. Boyer, 1994: *World Ocean Atlas 1994,* Vol. 4:*Temperature. NOAA Atlas NESDIS 4,* NOAA, U.S. Dept. of Commerce, 117 pp.

—— , S. R. Burgett, and T. P. Boyer, 1994: *World Ocean Atlas 1994,* Vol. 3: *Salinity. NOAA Atlas NESDIS 3,* NOAA U.S. Dept. of Commerce, 99 pp.

Lin, C. A., 1988: A mechanistic model of isopycnal diffusion in the ocean. *Climate Dyn.,* **2,** 165–171.

Manabe, S., and R. J. Stouffer, 1994: Multiple-century response of a coupled ocean–atmosphere model to an increase of atmospheric carbon dioxide. *J. Climate,* **7,** 5–23. Find this article online

Marotzke, J., and P. Stone, 1995: Atmospheric transports, the thermohaline circulation, and flux adjustments in a simple coupled model. *J. Phys. Oceanogr.,* **25,** 1350–1364. Find this article online

McDougall, T. J., 1987: Neutral surfaces. *J. Phys. Oceanogr.,* **17,** 1950–1964. Find this article online

—— , and J. A. Church, 1986: Pitfalls with the numerical representation of isopycnal and diapycnal mixing. *J. Phys. Oceanogr.,* **16,** 196–199. Find this article online

Montgomery, R. B., 1940: The present evidence on the importance of lateral mixing processes in the ocean. *Bull. Amer. Meteor. Soc.,* **21,** 87–94. Find this article online

Power, S. B., and A. C. Hirst, 1997: Eddy parameterization and the oceanic response to global warming. *Climate Dyn.,* **13,** 417–428.

Redi, M. H., 1982: Oceanic isopycnal mixing by coordinate rotation. *J. Phys. Oceanogr.,* **12,** 1154–1158. Find this article online

Robitaille, D. Y., and A. J. Weaver, 1995: Validation of sub-grid-scale mixing schemes using CFCs in a global ocean model. *Geophys. Res. Lett.,* **22,** 2917–2920.

Sausen, R., R. Barthels, and K. Hasselman, 1988: Coupled ocean–atmosphere models with flux correction. *Climate Dyn.,* **2,** 154–163.

Schmittner, A., and T. F. Stocker, 1999: The stability of the thermohaline circulation in global warming experiments. *J. Climate,* **12,** 1117–1133. Find this article online

—— , C. Appenzeller, and T. F. Stocker, 2000a: Enhanced Atlantic freshwater export during El Niño. *Geophys. Res. Lett.,* **27,** 1163–1166.

—— , —— , and —— , 2000b: Validation of parameterizations of the hydrological cycle used in zonally averaged climate models. *Climate Dyn.,* **16,** 63–77.

Shine, K. P., R. G. Derwent, D. J. Wuebbles, and J.-J. Morcrette, 1995: Radiative forcing of climate. *Climate Change, The IPCC Scientific Assessment,* J. T. Houghton, G. J. Jenkins, and J. J. Ephraums, Eds., Cambridge University Press, 41–68.

Stocker, T. F., and D. G. Wright, 1996: Rapid changes in ocean circulation and atmospheric radiocarbon. *Paleoceanography,* **11,** 773–796.

—— , and A. Schmittner, 1997: Influence of CO_2 emission rates on the stability of the thermohaline circulation. *Nature,* **388,** 862–865.

—— , D. G. Wright, and W. S. Broecker, 1992a: The influence of high-latitude surface forcing on the global thermohaline circulation. *Paleoceanography,* **7,** 529–541.

—— , —— , and L. A. Mysak, 1992b: A zonally averaged, coupled ocean–atmosphere model for paleoclimate studies. *J. Climate,* **5,** 773–797. Find this article online

Toole, J. M., K. L. Polzin, and R. W. Schmitt, 1994: Estimates of diapycnal mixing in the abyssal ocean. *Science,* **264,** 1120–1123.

Trenberth, K. E., and A. Solomon, 1994: The global heat balance: Heat transport in the atmosphere and ocean. *Climate Dyn.,* **10,** 107–134.

Tziperman, E., 1997: Inherently unstable climate behaviour due to weak thermohaline ocean circulation. *Nature,* **386,** 592–595.

Visbeck, M., J. Marshall, and T. Haine, 1997: Specification of eddy transfer coefficients in coarse-resolution ocean circulation models. *J. Phys. Oceanogr.,* **27,** 381–402. Find this article online

Weaver, A. J., and M. Eby, 1997: On the numerical implementation of advection schemes for use in conjunction with various mixing parameterizations in the GFDL ocean model. *J. Phys. Oceanogr.,* **27,** 369–377. Find this article online

Wiebe, E. C., and A. J. Weaver, 1999: On the sensitivity of global warming experiments to the parameterisation of sub-grid scale ocean mixing. *Climate Dyn.,* **15,** 875–893.

Wright, D. G., 1996: An equation of state for use in ocean models: Eckart's formula revisited. *J. Atmos. Oceanic Technol.,* **14,** 735–740.

—— , and T. F. Stocker, 1991: A zonally averaged ocean model for the thermohaline circulation. Part I: Model development and flow dynamics. *J. Phys. Oceanogr.,* **21,** 1713–1724. Find this article online

—— , and —— , 1992: Sensitivities of a zonally averaged global ocean circulation model. *J. Geophys. Res.,* **97,** 12 707–12 730.

—— , and —— , 1993: Younger Dryas experiments. *Ice in the Climate System,* W. R. Peltier, Ed., NATO ASI Series, Vol. I 12, Springer-Verlag, 395–416.

—— , C. B. Vreugdenhil, and T. M. Hughes, 1995: Vorticity dynamics and zonally averaged ocean circulation models. *J. Phys. Oceanogr.,* **25,** 2141–2154. Find this article online

—— , T. F. Stocker, and D. Mercer, 1998: Closures used in zonally averaged ocean models. *J. Phys. Oceanogr.,* **28,** 791–804. Find this article online
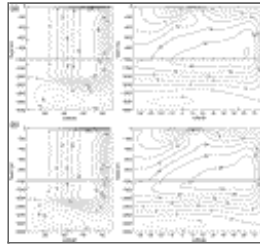
Tables

Table 1. Parameter values for the horizontal (K_H), vertical (K_V), isopycnal (K_I) and diapycnal (K_D) diffusivity (all in units m^2 s^{-1}), the Gent–McWilliams parameter κ (m^2 s^{-1}), the maximum isopycnal slope s_{max} (1), and the parameter for Southern Ocean deep water formation q_{SO} (Sv) used for the reference states of the different experiementss. HOR, ISO, and GM indicate horizontal mixing, isopycnal mixing, and the Gent–McWilliams parameterization, respectively

Click on thumbnail for full-sized image.

Figures

Click on thumbnail for full-sized image.

Fig. 1. Total Southern Ocean (left column) and Atlantic (right column) streamfunction (Sv) in the modern steady state, shown for (a) horizontal mixing (HOR), (b) isopycnal mixing (ISO), and (c) the Gent–McWilliams parameterization (GM). (d) the eddy-induced overturning
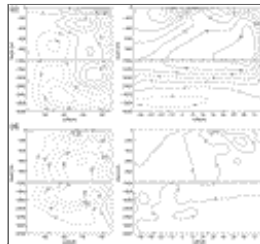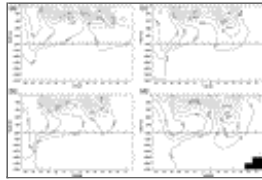

Click on thumbnail for full-sized image.

Fig. 1. (*Continued*) (Sv) for GM. Contour interval is 4 Sv (a–c and d, left panel) and 2 Sv (d, right panel), respectively. Note that the Southern Ocean extends around the globe and that the overturning transport is therefore not continuous where it meets the Atlantic
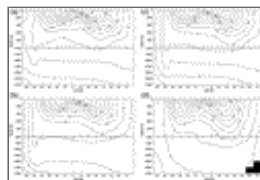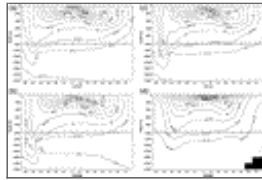

Click on thumbnail for full-sized image.

Fig. 2. Atlantic and Southern Ocean temperature distribution (°C) in the modern steady state shown for (a) horizontal mixing (HOR), (b) isopycnal mixing (ISO) and (c) the Gent–McWilliams parameterization (GM). Zonally averaged data from Levitus and Boyer (1994) is given in (d) for comparison
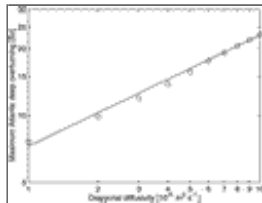
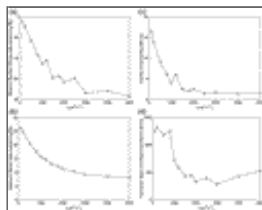Click on thumbnail for full-sized image.

Fig. 3. Atlantic and Southern Ocean salinity distribution in the modern steady state, shown for (a) horizontal mixing (HOR), (b) isopycnal mixing (ISO) and (c) the Gent–McWilliams parameterization (GM). Zonally averaged data from Levitus et al. (1994) is given in (d) for comparison

Click on thumbnail for full-sized image.

Fig. 4. Atlantic and Southern Ocean distribution of the density −1000 (kg m^{-3}) in the modern steady state, shown for (a) horizontal mixing (HOR), (b) isopycnal mixing (ISO), and (c) the Gent–McWilliams parameterization (GM). Zonally averaged data calculated from Levitus et al. (1994) and Levitus and Boyer (1994) is given in (d) for comparison
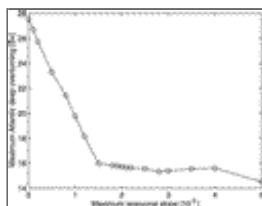
Click on thumbnail for full-sized image.

Fig. 5. Log–log plot of the maximum deep overturning in the Atlantic as a function of the diapycnal diffusivity K_D. A line proportional to $(K_D)^{0.5}$ is drawn for comparison
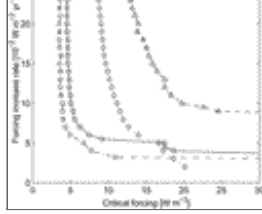
Click on thumbnail for full-sized image.

Fig. 6. (a) Minimum Southern Ocean eddy-induced overturning (indicating the strength of the Southern Ocean overturning cell), (b) maximum total Atlantic overturning (including eddy-overturning), (c) fraction of convecting cells in World Ocean, and (d) convection depth in northernmost Atlantic cell (65°–80°N) as a function of the Gent–McWilliams parameter κ.
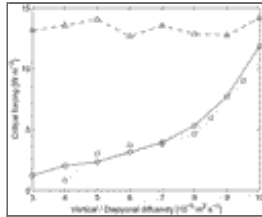
Click on thumbnail for full-sized image.

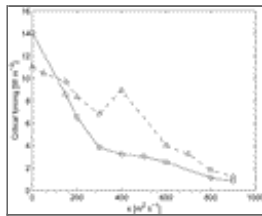Fig. 7. Maximum total Atlantic overturning as a function of the maximum isopycnal slope

Click on thumbnail for full-sized image.

Fig. 8. Critical additional radiative forcing for the collapse of the Atlantic thermohaline circulation as a function of the increase rate of the additional radiative forcing. The results for horizontal mixing (circles), isopycnal mixing (triangles), the Gent–McWilliams parameterization (squares), and the corresponding curve for horizontal mixing of Schmittner and Stocker (1999, Fig. 20b, P1A0ad) (diamonds) are plotted. The uncertainty in the model estimates of the critical forcing threshold values is negligible (± 0.05 W m^{-2})

Click on thumbnail for full-sized image.

Fig. 9. Critical additional radiative forcing for the collapse of the Atlantic thermohaline circulation as a function of the diapycnal or vertical diffusivity. The results for horizontal mixing (circles), isopycnal mixing (triangles), and the GM parameterization (squares) are plotted. The uncertainty in the model estimates of the critical forcing threshold values is ± 0.05 W m^{-2}

Click on thumbnail for full-sized image.

Fig. 10. Critical additional radiative forcing for the collapse of the Atlantic thermohaline circulation as a function of the Gent–McWilliams parameter κ for the standard deep water parameterization in the Southern Ocean (GM: circles) and for a parameterization with reduced deepwater formation in the Southern Ocean (GM2: triangles). The uncertainty in the model estimates of the critical forcing threshold values is ± 0.05 W m^{-2}

Corresponding author address: Dr. Thomas F. Stocker, Climate and Environmental Physics, Physics Institute, University of Bern, Sidlerstrase 5, CH-3012 Bern, Switzerland.

E-mail: stocker@climate.unibe.ch

top ▲